*Desalination and Water Treatment*
www.deswater.com

doi: 10.5004/dwt.2020.25615

189 (2020) 428–439
June

# Application of *Dimocarpus longan* ssp. *malesianus* leaves in the sequestration of toxic brilliant green dye

Amal Asheeba Romzi[a], Linda B.L. Lim[a,*], Chin Mei Chan[a], N. Priyantha[b,c]

[a]*Chemical Sciences Programme, Faculty of Science, Universiti Brunei Darussalam, Negara Brunei Darussalam, Tel. +673 8748010; emails: linda.lim@ubd.edu.bn (L.B.L. Lim) asheeba.romzi@gmail.com (A.A. Romzi), chinmei.chan@ubd.edu.bn (C.M. Chan)*
[b]*Department of Chemistry, Faculty of Science, University of Peradeniya, Sri Lanka, email: namal.priyantha@yahoo.com (N. Priyantha)*
[c]*Postgraduate Institute of Science, University of Peradeniya, Peradeniya, Sri Lanka*

Received 2 August 2019; Accepted 25 January 2020

**ABSTRACT**

Recent years have seen the rise in the use of leaf-based adsorbents to remove pollutants. Not only are leaves low-cost and abundant, but they also contain many compounds giving rise to various functional groups that could promote the adsorption process. This study focuses on the use of leaves of *Dimocarpus longan* ssp. *malesianus* var. *malesianus*, locally known as "mata kuching" and literally translated as "cat's eyes", as an adsorbent for the removal of toxic brilliant green (BG) dye. The mata kuching leaves (MKL) reached equilibrium when in contact with BG dye within 30 min. Its adsorption toward BG was not greatly affected by varying pH solutions or salt concentrations. Of the five models tested, the Sips model was the best fit for the adsorption isotherm data, giving a maximum adsorption capacity of 337.9 mg $g^{-1}$. Adsorption process followed the pseudo-second-order kinetics and intraparticle diffusion was not the rate-controlling step. Regeneration and reuse of spent MKL were possible especially when treated with a base, maintaining almost 80% dye removal at the 5th consecutive cycle. With its many attractive features such as high adsorption capacity, short contact time, ability to be regenerated, relative stability under varying conditions, availability in abundance throughout the year, MKL, therefore, has potential application as a low-cost adsorbent in wastewater treatment.

*Keywords:* Leaf adsorbent; Adsorption isotherm; Brilliant green dye; Kinetics; Thermodynamics; Regeneration

## 1. Introduction

The advancement of technology in this modern era has led to a boom in industries to cater to the needs of the rising world population. The use of colors plays an important role in marketing products to attract consumers. In fact, colors are a major part of our lives. Ever since the discovery of mauve, the first dye to be synthesized back in the mid-19th century, many dyes have since been synthesized. The limitations of natural dyes and the demand for inexpensive and readily available synthetic dyes saw the commercial decline of natural dyes. Synthetic dyes are heavily used in industries such as textiles, paint, and printing. Wastewater containing dye effluents is now one of the major pollutions faced by the world today. Not only do they give rise to non-aesthetic pollution, but these dyes also produce harmful by-products and cause eutrophication. Synthetic dyes are usually non-biodegradable and their prolong presence in water bodies leads to foul smell, affects sunlight penetration and has harmful toxic effects to aquatic life. Through the food chain, this will also have detrimental effects on human health [1,2]. Hence, cleaning up wastewater is not an option but a necessity.

One of the methods of wastewater treatment that has received much attention is through the use of adsorption. Compared to many methods, adsorption is attractive in that it is economically viable since it utilizes low-cost, readily available materials and the method is straight forward

* Corresponding author.

requiring no complicated skills [3,4]. Many natural adsorbents have been reported and examples include wastes from industries and agriculture [5–7], soil materials [8,9] and aquatic plants [10]. Modified adsorbents through physically or chemically means, as well as synthetic adsorbents, have also been tested out for their adsorption ability [11,12]. Not all adsorbents showed good adsorption of dyes [13,14]. Therefore there is still a demand for the continual search for good low-cost adsorbents which could be of potential use in the treatment of wastewater.

Brilliant green (BG) belongs to the triphenylmethane dyes and is closely related to the malachite green dye. In fact, BG is sometimes known as malachite green G dye. The triphenylmethane dyes are known to have carcinogenic and genotoxic properties [15]. Being intensely colored, BG has been used in the textile industry to dye wool and silk as well as in the paper industry to color papers [16]. BG was found to exhibit inhibition against gram-positive bacteria and when ingested, BG is known to cause abdominal pain, diarrhea, and vomiting [17]. Although BG is used as a local antiseptic [18], it is rendered toxic when ingested and if in contact with eyes, BG may cause corneal opacification, which can lead to blindness [19]. Its exposure, be it direct or indirect, can also cause harm to humans [20]. Hence, its removal from wastewater is of crucial importance.

The use of leaves as natural adsorbents has gained popularity over the years because they are easily obtainable in large quantities throughout the year. Examples include tea leaves [21], leaves of *Artocarpus odoratissimus* [22], *Bilimbi*, *Eucalyptus* [23], *Citrus grandis* (pomelo) [24] and many others [25], all of which have been successfully reported to adsorb dyes or heavy metals. Here, we report the use of leaves of *Dimocarpus longan* ssp. *malesianus* var. *malesianus* as an adsorbent for the removal of BG in simulated wastewater. *Dimocarpus longan* ssp. *malesianus* var. *malesianus* is native to Southeast Asia with the greatest diversity being found in Borneo [26]. It belongs to the family of *Sapindaceae* and is known by the local Malays as "mata kuching" which is literally translated as "cat's eyes". The tree bears fruits that are round with a rough, light brownish skin, similar in size to its close relative, the more widely known *Euphoria longana* (Longan). Mata kuching leaves (MKL) have been found to exhibit xanthine oxidase inhibitory activity. MKL, therefore, has the potential to treat gout since xanthine oxidase inhibitors can block uric acid biosynthesis from purine in the body [27].

This paper focuses on the use of MKL as a natural adsorbent for the removal of BG dye. The adsorption characteristics of MKL toward BG dye such as contact time, isotherm, kinetics, stability in varying pH and salt conditions, and its ability to be regenerated will be investigated. The results obtained from this work will help to shed light on the potential of MKL as a new adsorbent in the treatment of wastewater containing BG dye.

## 2. Materials and methods

### 2.1. Chemicals and instrumentations

All the chemicals and reagents used in this study were used with no further purification. The brilliant green (BG) dye ($C_{27}H_{34}N_2O_4S$, $M_r$ 482.63 g mol$^{-1}$) was obtained from Sigma-Aldrich, Paris. The 1,000 mg L$^{-1}$ BG stock solution was prepared by adding distilled water to dissolve the needed amount of dye. The pH was altered by using 0.1 mol L$^{-1}$ HCl and 0.1 mol L$^{-1}$ NaOH. Sodium chloride and potassium nitrate were used in the investigation of ionic strength and point of zero charge, respectively. Throughout this study, distilled water was used.

The absorbance of the BG dye solutions was measured with the Shimadzu UV-1601PC UV-visible spectrophotometer (UV-Vis), Japan, set at wavelength 624 nm. The functional groups of MKL were identified through the KBr method using the Shimadzu IR Prestige-21 spectrophotometer for Fourier transform infrared spectroscopy (FTIR) analysis. Scanning electron microscope (SEM), JSM-7610F JOEL model (USA), provided the surface morphology of the samples.

### 2.2. Sample preparation

MKL was collected from a local garden. The leaves were separated from the twigs and branches and collected into a pile. To remove any dirt particles, the leaves were washed with distilled water and dried in the oven at 60°C until a constant weight was achieved. The dried leaves were then blended to powder form and sieved using laboratory sieve to acquire particles of a diameter of less than 355 μm.

### 2.3. Optimization of parameters and batch adsorption experiments

All experiments were conducted by mixing 0.020 g of MKL powder with 10.0 mL of known concentration of BG dye solution (mass to volume ratio fixed at 1:500) in clean 125 mL of a conical flask unless otherwise stated. Using an orbital shaker, the mixtures were then agitated at 250 rpm, at room temperature, except for investigation of thermodynamics studies in which the experiments were carried out with temperatures ranging from 298 to 343 K. Experimental parameters for the effects of contact time (30 min intervals for up to 2 h), pH (4–10), ionic strength (0.1–0.8 M NaCl) were investigated, following the methods as outlined by Zaidi et al [28]. Also included in the study was kinetics using a 100 mg L$^{-1}$ BG solution. Batch adsorption isotherm experiments were performed with BG dye concentrations ranging from 0 to 1,000 mg L$^{-1}$.

The amount of dye adsorbed per gram of MKL, $q_e$ (mmol g$^{-1}$), was calculated using:

$$q_e = \frac{\left(C_i - C_e\right)V}{M_r m} \tag{1}$$

where $C_i$ is the initial concentration of the dye (mg L$^{-1}$), $C_e$ is the equilibrium of the concentration of the dye (mg L$^{-1}$), $M_r$ is the dye molecular mass (mol g$^{-1}$), $V$ is the volume of the BG solution used (L), and $m$ is the mass of MKL used in this experiment (g).

The percentage removal of the dye can be known using:

$$\text{Percentage removal} = \frac{\left(C_i - C_e\right)\times 100\%}{C_i} \tag{2}$$

### 2.4. Determination of point zero charge

The point of zero charge ($pH_{pzc}$) of MKL was determined using 0.1 mol $L^{-1}$ of $KNO_3$ solution as outlined by Chieng et al [29] with pH ranging from 2 to 10. Adjustment of the pH of the salt solution was done using 0.1 mol $L^{-1}$ HCl and 0.1 mol $L^{-1}$ NaOH. The pH adjusted salt solutions, each containing MKL, were agitated for 24 h and the final pH was recorded.

### 2.5. Error analysis

In this study, error functions were used to provide information on the suitability of the kinetics and isotherm models. The six error functions used are the sum of absolute error (EABS), the average relative error (ARE), the Marquart's percent standard deviation (MPSD), sum square error (EERSQ), hybrid fractional error function (HYBRID) and chi-square test ($\chi^2$) and their equations are shown as Eqs. (3)–(8), respectively. The models with smaller error values are better fitted to experiment data [30].

$$\text{EABS: } \sum_{i=1}^{p}\left|q_{e,\text{meas}}-q_{e,\text{calc}}\right| \tag{3}$$

$$\text{ARE: } \frac{100}{p}\sum_{i=1}^{p}\left|\frac{q_{e,\text{meas}}-q_{e,\text{calc}}}{q_{e,\text{calc}}}\right|_i \tag{4}$$

$$\text{MPSD: } 100\sqrt{\frac{1}{p-n}\sum_{i=1}^{p}\left(q_{e,\text{meas}}-q_{e,\text{calc}}\right)^2} \tag{5}$$

$$\text{EERSQ: } \sum_{i=1}^{n}\left(q_{e,\text{calc}}-q_{e,\text{meas}}\right)_i^2 \tag{6}$$

$$\text{HYBRID: } \frac{100}{n-p}\sum_{i=1}^{n}\left[\frac{\left(q_{e,\text{meas}}-q_{e,\text{calc}}\right)^2}{q_{e,\text{meas}}}\right]_i \tag{7}$$

$$\chi^2\text{: } \sum_{i=1}^{p}\frac{\left(q_{e,\text{meas}}-q_{e,\text{calc}}\right)^2}{q_{e,\text{meas}}} \tag{8}$$

where $q_{e,\text{meas}}$ is the value of the experiment while $q_{e,\text{calc}}$ is the value calculated from the isotherm models and $p$ is the number of observations in the experiment.

## 3. Results and discussion

### 3.1. Characterization of MKL

#### 3.1.1. Functional group characterization

The functional groups on the surface of MKL, especially those involved in the adsorption of BG dye, were determined using FTIR spectroscopy. Broad O–H and N–H stretching at 3,421 $cm^{-1}$, C=O stretch at 1,516 $cm^{-1}$ and C–O–H stretch at 1,047 $cm^{-1}$ were shifted upon adsorption of BG dye, as shown in Fig. 1. Similarly, the C=O peak at 1,732 $cm^{-1}$ in MKL appeared shifted to 1,742 $cm^{-1}$. A weak peak at 1,833 $cm^{-1}$ could be C=O of anhydride and this was shifted to 1,815 $cm^{-1}$ after BG was being adsorbed. The C=C at 1,620 $cm^{-1}$ remained unaffected. Aromatic and aliphatic C–N stretching absorptions of BG dye at 1,276 and 1,188 $cm^{-1}$, respectively, are being detected in the spectrum of the dye loaded MKL, further confirming that BG was successfully adsorbed onto MKL [31]. Generally, leaves contain various compounds such as cellulose, lignin, hemicellulose, pectin, etc. Their functional groups such as O–H, C=O, N–H, could act as binding sites in the removal of adsorbates [25].

#### 3.1.2. Surface morphology of MKL

SEM images provided insight into the surface morphology of MKL, before and after adsorption of BG dye. Before the adsorption of BG dye, the surface of MKL appeared irregular and consists of many folds in various shapes and sizes (Fig. 2). When loaded with BG dye, there was a notable change in the surface morphology of MKL. These irregular shapes and cavities now appeared to be covered with dye, making the surface much smoother and flat, showing clear evidence of adsorption of BG dye onto the surface of MKL. Similar observations have also been previously reported upon adsorption of dyes onto the surface of adsorbents [32].

#### 3.1.3. Point of zero charge of MKL

In surface science, the point of zero charge ($pH_{pzc}$) is of fundamental importance as it is the pH at which an adsorbent's surface has zero net charge that is, neutral. Useful information, especially on the ionization of surface functional groups, can be derived thereby helping in the prediction of interactions of surface functional groups with ions in solution. When solution pH > $pH_{pzc}$, the surface of the adsorbent will be predominately negative as a result of the deprotonation of surface functional groups, whereas when solution pH < $pH_{pzc}$, the surface of the adsorbent is predominately positive [12]. In general, the negatively charged surface will attract positively charged molecules or ions and the reverse is true that is, a positively charged surface will attract negatively charged molecules or ions through electrostatic interactions. As shown in Fig. 3, $pH_{pzc}$ (the point intercepting the *x*-axis) for MKL was found to be at pH 4.69, a value lower than *Nephelium mutabile* leaf (5.29) [33], tea waste (6.6) [34], *Cinnamomum camphora* leaves (5.9) [35], pomelo leaf (5.02) [24], *Artocarpus odoratissimus* leaf (6.2) [22], except for *Nepenthes* leaf (3.9) [36] and *Gliricidia sepium* leaf (2.0) [37].

### 3.2. Optimization of adsorption parameters

#### 3.2.1. Effect of contact time

It is important to have information on the contact time in an adsorption process as the data obtained will be useful in determining the length of time required for the adsorbate-adsorbent system to achieve the state of equilibrium. Fig. 4 shows the effect of contact time on the removal of BG dye by MKL. The rate of the removal of BG dye increased sharply during the initial 30 min and equilibrated within half an hour of contact time. The rapid increase in the percentage of the removal of BG observed in the first 30 min

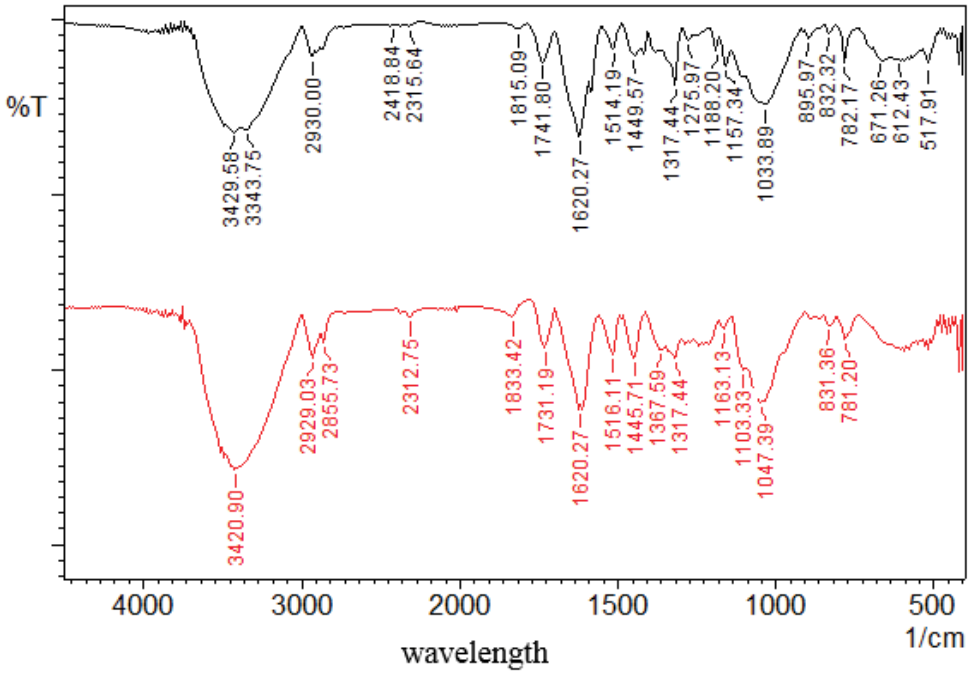


Fig. 1. FTIR spectra of MKL before (red) and after (black) adsorption of BG.

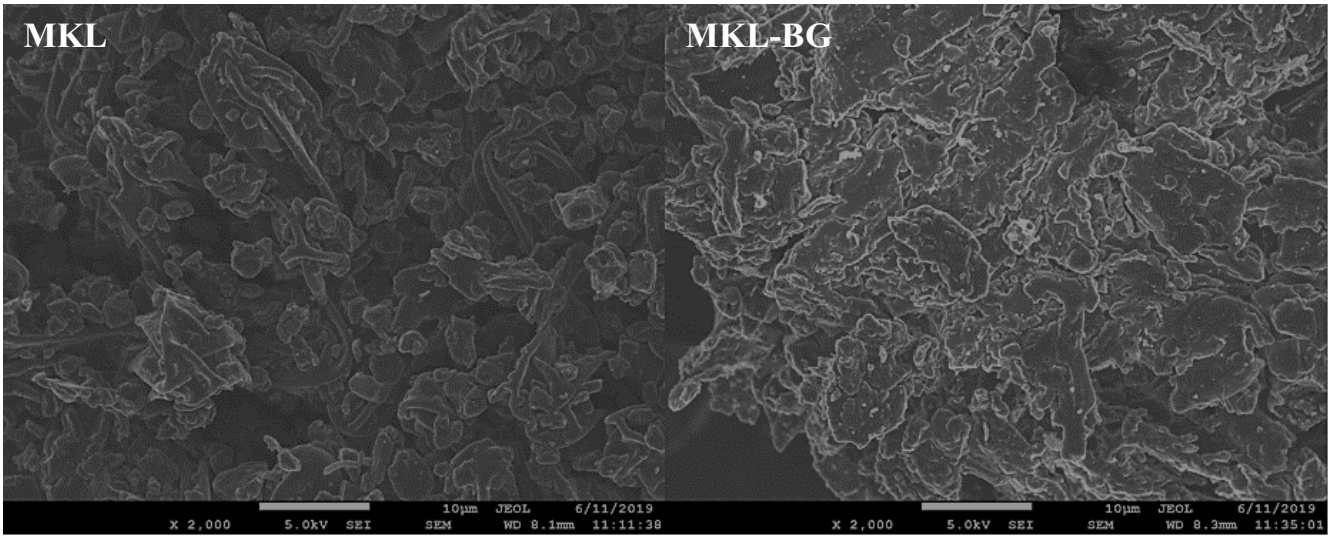


Fig. 2. SEM images of MKL before and after adsorption of BG at 2,000× magnification.

is due to the abundance of active vacant sites on the surface of MKL, which allow BG dye molecules to be quickly adsorbed. As these vacant sites are being filled, the adsorbed dyes result in the sites becoming more and more saturated. Hence, the adsorption process slows down and finally levels off to a plateau upon reaching equilibrium. A short period of time for an adsorbent-adsorbate system to reach equilibrium is an attractive feature in designing wastewater treatment via the adsorption method. This will help save cost and time, which are crucial in any operation of a treatment plant. Based on the results obtained, half an hour of contact time was sufficient for the MKL-BG system to reach equilibrium. Hence, all subsequent reactions, except for kinetics study, were carried out by shaking the adsorbent-adsorbate system for half an hour.

### 3.2.2. Effect of pH on MKL's adsorption of BG

The effect of pH is an important parameter in adsorption study because the pH of wastewater will not be neutral nor constant at all times due to the presence of many different pollutants and electrolytes. Further, many dyes are sensitive to pH and the presence of acids or bases can result in protonation or deprotonation of the functional

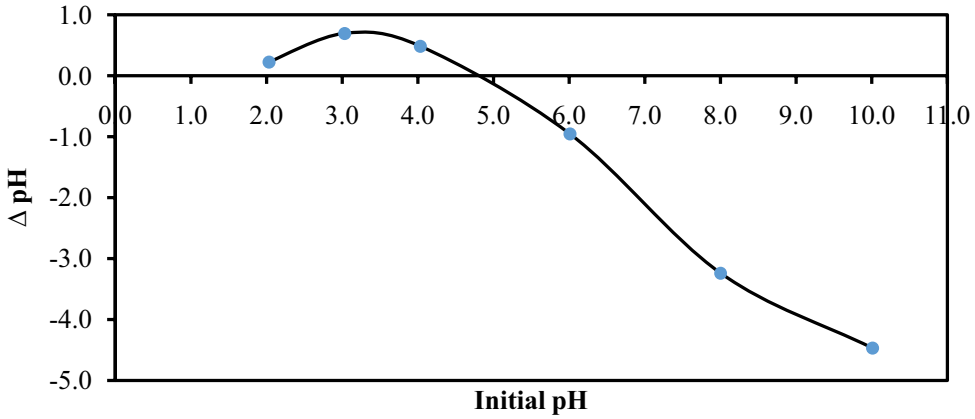


Fig. 3. Determination of point of zero charge of MKL.

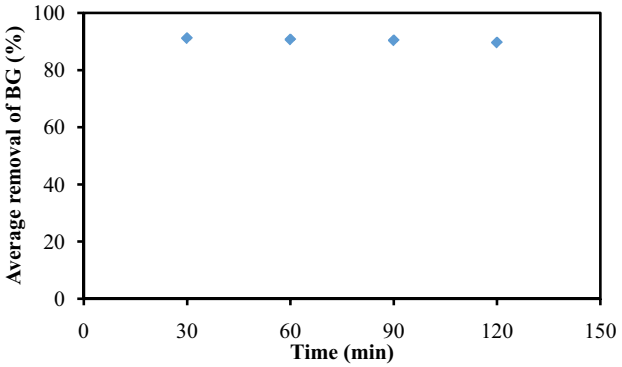


Fig. 4. Effect of contact time on the removal of 100 mg $L^{-1}$ BG dye by MKL.

groups present in both the dyes and adsorbent. In this study, the investigation of the effect of pH on MKL's adsorption toward BG was kept in the range of pH 4 to 10 to avoid any changes that may cause fading of the intensity of the dye color thereby resulting in inaccuracy of the results [12]. As shown in Fig. 5, the adsorption of BG dye onto MKL was not affected much by the change of pH when compared to the untreated (natural) pH for BG dye at pH 3.8. The highest adsorption was at pH 4, with 86% removal, and the lowest at pH 10 (66%). The adsorption of BG dye at natural pH was 78%. For an adsorbent to be applicable in wastewater treatment, it has to remain stable and show resilience toward pH changes by still being able to remove the dye. Many adsorbents have been reported to show a drastic reduction in their ability to remove dyes when the pH is being altered. Hence, in this aspect, it can be concluded that MKL is a relatively good adsorbent given its ability to remove BG under varying pH changes. Even though the removal of BG was the highest at pH 4, however when compared to removal of BG at the natural pH it only differed by 8%. Hence, all subsequent experiments were carried out without any pH adjustments.

### 3.2.3. Effect of ionic strength

The presence of ions in wastewater can affect the process of adsorption of adsorbates such as dye molecules. This is because electrostatic and hydrophobic-hydrophobic interactions can be affected by ionic strength [38]. Non-polar groups such as $-CH_3$ group of the dye can react with aromatic ring present on the surface of the adsorbent in an interaction called hydrophobic–hydrophobic interaction. The electrostatic attraction mechanism of cationic dyes in high ionic strength solutions can be repressed because of the metal ions competing with it for the active sites on the surface of the adsorbent, leading to electrostatic repulsion.

In Fig. 6 it can be seen how different concentrations of NaCl affect the adsorption of the BG dye by MKL. A gradual decreasing trend was observed as the concentration of the NaCl increases, with a reduction of 20% in MKL's adsorption capability toward BG in 1.0 M NaCl. This can be attributed to the presence of high $Na^+$ ions which not only can cause electrostatic repulsion with the cationic BG dye but also compete for the available vacant active sites on the surface of MKL. Such behavior is quite common for the removal of the basic dye and has been reported in many studies [39,40]. Unlike many adsorbents whose adsorption capacity is drastically affected by ionic strength [32,41], the results obtained from this study suggest MKL to be relatively resilient to an increase in salt concentration. Hence, MKL could be a possible candidate to be used in real wastewater as the industrial effluents usually have high salt content.

### 3.2.4. Adsorption kinetics of BG onto MKL

The study of the kinetics of adsorption of the BG dye by the MKL was investigated to gain insight into the mechanism's process. Two kinetics models were applied to the experimental data namely, the Lagergren pseudo-first-order [42] and pseudo-second-order [43]. Their linearized equations are represented by Eqs. (9) and (10), respectively.

$$\log\left(q_e - q_t\right) = \log q_e - \frac{t}{2.303}k_1 \tag{9}$$

$$\frac{t}{q_t} = \frac{1}{q_e^2 k_2} + \frac{t}{q_e} \tag{10}$$

where $q_t$ is the amount of the adsorbed by the adsorbate per gram of adsorbent (mmol $g^{-1}$) at time $t$, $k_1$ is the

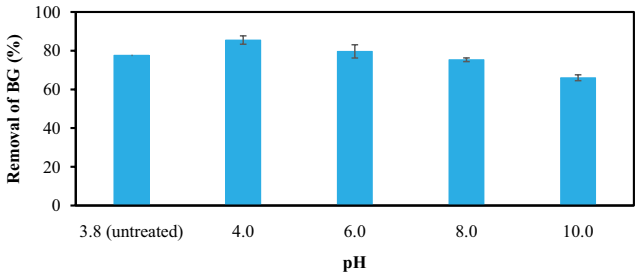


Fig. 5. Effect of adsorption of BG by MKL in different pH.

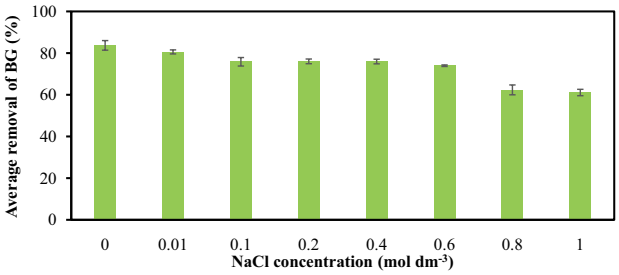


Fig. 6. Adsorption of BG dye onto MKL in different concentrations of NaCl.

Lagergren-first-order rate constant ($min^{-1}$), $t$ is the time of shaking (min) and $k_2$ is a pseudo-second-order rate constant (g $mmol^{-1}$ $min^{-1}$).

It can be observed from Table 1 that of the two models employed, the pseudo-second-order kinetics is a better fit in terms of its higher $R^2$ (0.9996), compared to the Lagergren pseudo-first ($R^2$ = 0.3265). Analyses of these models using six different error functions also confirmed that the adsorption of BG by MKL followed the pseudo-second-order kinetics as indicated by its overall small error values (Table 1). The experiment adsorption capacity ($q_{exp}$) was determined to be 0.088 mmol $g^{-1}$ which supported the calculated adsorption capacity ($q_{calc}$) for pseudo-second-order but not for the Lagergren pseudo-first-order. Comparison of the experiment kinetics data with the two simulated kinetics models, as depicted in Fig. 7, once again point to the pseudo-second-order kinetics being the better fit model for the adsorption of BG onto MKL.

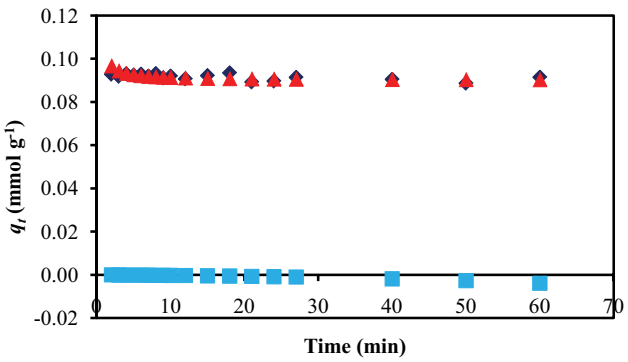


Fig. 7. Comparison of experiment data (◆) with simulated plots of pseudo-first-order (■) and pseudo-second-order (▲).

The adsorbate transfer of the solid–liquid sorption process is frequently categorized by the external diffusion (which is also known as film diffusion), surface diffusion, and pore diffusion or joint surface and pore diffusion. Unfortunately, the Lagergren pseudo-first-order and the pseudo-second-order kinetics models do not give any information on the diffusion process. Hence, the Weber–Morris intra-particle model [44] was deployed and its equation is shown below in Eq. (11).

$$q_t = k_i t^{1/2} + C \tag{11}$$

where $k_i$ is the intra-particle diffusion rate constant (mg $g^{-1}$ $min^{-1/2}$) and $C$ is the intercept.

The intra-particle diffusion model is beneficial in calculating the rate-controlling step and recognizing the mechanism of the adsorption and the pathways of the reaction. If the plot of $q_t$ against $t^{0.5}$ passes through the origin and is linear, it is acknowledged that the adsorption is ruled by intra-particle diffusion wholly. The adsorption process can be governed by a multistep mechanism if multiple linear regions are obtained from the intra-particle diffusion plot. The multistep mechanisms can be broken down into four steps related to the processes of the transport during adsorption by porous adsorbents. The first stage is the solution phase's transport which is known as bulk transport and it can happen immediately after the transfer process of the adsorbent into the solution of

Table 1
Kinetics parameters and error values of Lagergren pseudo-first-order and pseudo-second-order models

| Model | | ARE | EERSQ | HYBRID | EABS | MPSD | $\chi^2$ |
|---|---|---|---|---|---|---|---|
| Pseudo-first-order | | 100.82 | 0.16 | 10.40 | 1.75 | 106.59 | 1.77 |
| $k_1$ ($min^{-1}$) | –0.03 | | | | | | |
| $q_{calc}$ (mmol $g^{-1}$) | 0.001 | | | | | | |
| $R^2$ | 0.3265 | | | | | | |
| Pseudo-second-order | | 1.90 | 0.00 | 0.01 | 0.03 | 3.73 | 0.00 |
| $k_2$ (g $mmol^{-1}$ $min^{-1}$) | 1102.62 | | | | | | |
| $q_{calc}$ (mmol $g^{-1}$) | 0.090 | | | | | | |
| $R^2$ | 0.9996 | | | | | | |
| $q_{exp}$ (mmol $g^{-1}$) | 0.088 | | | | | | |

the adsorbate and hence the control engineering design is not controlled by it. This stage happens too sudden and its contribution is considered insignificant. The second stage, known as film diffusion (occurs slowly). Through a hydrodynamic boundary layer or film, the molecules of the adsorbate are transported to the external surface of the adsorbent from the bulk liquid phase that occurs in this stage. The third stage includes the diffusion of the molecules of the adsorbate into the pores of the adsorbent from the adsorbent's exterior, along the pore-wall surfaces, or both (which is known as intra-particle diffusion, meaning it happens slowly). The fourth stage is the attachment of the adsorptive, which always happens rapidly; hence, it is negligible for the design also.

The Weber–Morris plot for the BG onto MKL in Fig. 8 shows a single linear plot that does not involve a multistep mechanism. The plot does not pass through the origin, indicating that intra-particle diffusion may not be the rate-controlling step in the adsorption process.

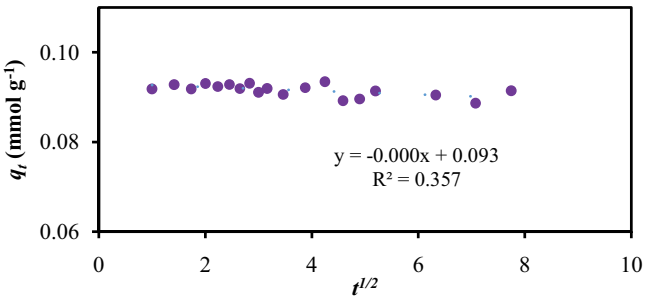


Fig. 8. Weber–Morris intra-particle diffusion plot for adsorption of BG onto MKL.

### 3.2.5. Adsorption isotherm

Adsorption isotherm provides insight into the adsorption's mechanism and gives information on the partition quantitative assessment or solutes distribution of interest at equilibrium between the fluid and solid phases. Accurate interpretation and comprehension of the adsorption isotherm are crucial for the effective design of the adsorption system and the complete improvement of the mechanism pathways of the adsorption. Five adsorption isotherm models (Table 2) were employed in this study to analyze the experimental data obtained. Since the linearization of

Table 2
Five isotherm models used in this study

| Isotherm model | Linearized equation | Plot |
|---|---|---|
| Langmuir [46] | $\frac{C_e}{q_e}=\frac{1}{K_L q_{\max}}+\frac{C_e}{q_{\max}}$<br>$K_L$ is the Langmuir constant<br>$R_L=\frac{1}{1+K_L C_0}$<br>$R_L$ is the dimensionless constant<br>$R_L$ range = $1.191\times10^{-01}$ – $9.978\times10^{-01}$ | $\frac{C_e}{q_e}$ vs $C_e$ |
| Freundlich [47] | $\log q_e=\frac{1}{n}\log C_e+\log K_F$<br>$K_F$ is the Freundlich constant indicative of adsorption capacity, $n$ is related to the adsorption intensity | $\log q_e$ vs $\log C_e$ |
| Temkin [48] | $q_e=\left(\frac{RT}{b_T}\right)\ln K_T+\left(\frac{RT}{b_T}\right)\ln C_e$<br>$K_T$ is the Temkin constant; $b_T$ is related to the heat of adsorption; $R$ is the gas constant and $T$ is the absolute temperature at 298 K | $q_e$ vs $\ln C_e$ |
| Redlich–Peterson (R–P) [49] | $\ln\left(\frac{K_R C_e}{q_e}-1\right)=\beta\ \ln C_e+\ln a_R$<br>$K_R$ and $a_R$ are the R–P constants | $\ln\left(\frac{K_R C_e}{q_e}-1\right)$ vs $\ln C_e$ |
| Sips [50] | $\ln\left(\frac{q_e}{q_{\max}-q_e}\right)=\frac{1}{n}\ln C_e+\ln K_s$<br>$K_S$ is the Sips constant and $n$ is the Sips exponent | $\ln\left(\frac{q_e}{q_{\max}-q_e}\right)$ vs $\ln C_e$ |

the isotherm models can result in inherent bias, the results for each model were also analyzed with six error functions (Table 3) [30]. Further confirmation of the best-fit isotherm was concomitantly carried out with non-linear isotherm plots (Fig. 9). Such plots are more relevant because the original isotherm equations are being used and hence any problems arising from the violation using linearized equations are taken care of [45].

Based on the regression coefficient $R^2$ values, the order from the highest to lowest models is as follows: Sips > Temkin > Langmuir > Freundlich > Redlich–Peterson. The exclusion of both the Freundlich and Redlich–Peterson can further be confirmed by their high error values and deviation from the experiment data (Fig. 9). Of the three models left, the Langmuir, which depicts monolayer adsorption onto a homogenous adsorbent surface, is less fitting than the Sips and Temkin models based on its slightly higher error values and lower $R^2$ value. It's dimensionless constant, otherwise known as separation factor ($R_L$), has values ranging from between 0.12 to 0.99, indicating a favorable adsorption process. Between the Sips and Temkin models, the former has higher $R^2$ value and the simulation plot seemed better fitted to the experiment data, even though the latter model's errors were slightly lower overall. The Temkin model takes into consideration the indirect adsorbate-adsorbent interactions during an adsorption process and thereby proposed a linear decrease in the heat of adsorption of molecules with an increase in coverage of the adsorbent's surface. The heat of adsorption $b_T$ is indicative of chemisorption.

One of the factors in determining whether an adsorbent will be suitable in its application in wastewater treatment is its adsorption capability. Over the years, many adsorbents have been tested out and not all adsorbents have the ability to remove pollutants satisfactory. Our present study showed that MKL when compared to many reported leaves, gave excellent maximum adsorption capacity ($q_{max}$) as shown in Table 4. Similarly, when compared to many natural adsorbents and even synthesized or chemically modified adsorbents, MKL also exhibited higher or comparable $q_{max}$ value.

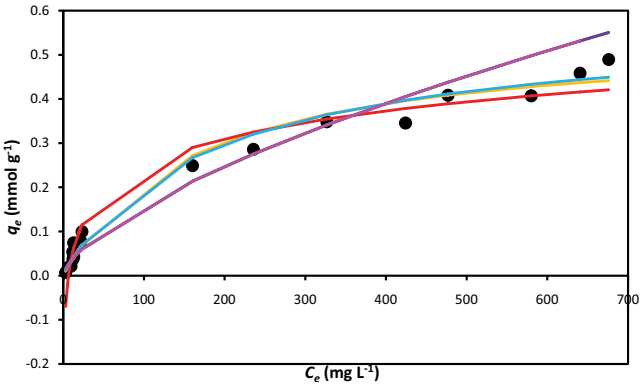


Fig. 9. Experiment isotherm data (●) with simulated plots of Langmuir (—), Freundlich (—), Temkin (—), R–P (—) and Sips (—).

Table 3
Parameter values and error analysis of the five adsorption isotherm models

| Model | Values | ARE | EERSQ | HYBRID | EABS | MPSD | $\chi^2$ |
|---|---|---|---|---|---|---|---|
| Langmuir | | 12.62 | 0.01 | 0.32 | 0.31 | 19.73 | 0.13 |
| $q_{max}$ (mmol g$^{-1}$) | 0.542 | | | | | | |
| $K_L$ (L mmol$^{-1}$) | 0.006 | | | | | | |
| $R^2$ | 0.9617 | | | | | | |
| Freundlich | | 15.28 | 0.01 | 0.41 | 0.38 | 24.81 | 0.18 |
| $K_F$ (mmol g$^{-1}$ (L mmol$^{-1}$)$^{1/n}$) | 0.010 | | | | | | |
| $n$ | 1.639 | | | | | | |
| $R^2$ | 0.9434 | | | | | | |
| Temkin | | 11.21 | 0.01 | 0.33 | 0.32 | 16.81 | 0.09 |
| $K_T$ (L mmol$^{-1}$) | 0.127 | | | | | | |
| $b_T$ (kJ mol$^{-1}$) | 26.09 | | | | | | |
| $R^2$ | 0.9654 | | | | | | |
| Redlich–Peterson | | 15.26 | 0.01 | 0.44 | 0.38 | 24.78 | 0.19 |
| $K_R$ (L g$^{-1}$) | 0.300 | | | | | | |
| β | 0.384 | | | | | | |
| $a_R$ (L mmol$^{-1}$) | 31.996 | | | | | | |
| $R^2$ | 0.8815 | | | | | | |
| Sips | | 11.87 | 0.01 | 0.26 | 0.22 | 22.11 | 0.13 |
| $q_{max}$ (mmol g$^{-1}$) | 0.700 | | | | | | |
| $K_S$ (L mmol$^{-1}$) | 0.009 | | | | | | |
| $1/n$ | 0.825 | | | | | | |
| $n$ | 1.213 | | | | | | |
| $R^2$ | 0.9696 | | | | | | |

Table 4
Comparison of $q_{max}$ values of MKL with leaves and some selected natural and synthetic adsorbents

| Adsorbent | $q_{max}$ (mg g$^{-1}$) | Reference |
|---|---|---|
| *Dimocarpus longan* ssp. *malesianus* leaves (MKL) | 261.8 (Langmuir) 337.9 (Sips) | This study |
| Leaves as adsorbents | | |
| *Psidium guajava* (Guava) leaves | 1.2 | [51] |
| Neem leaves | 70.9 | [52] |
| *Azadirachta indica* (Neem) leaves | 133.7 | [53] |
| *Nephelium mutabile* (Pulasan) leaves | 130.3 | [34] |
| *Saraca asoca* (Ashoka) leaves | 125.0 | [54] |
| *Eugenia jambolana* leaves | 4.7 | [55] |
| Base treated *Eugenia jambolana* leaves | 5.2 | [55] |
| Natural adsorbents | | |
| Rice husk ash | 21.6 | [56] |
| Pomelo skin | 325.0 | [57] |
| Bagasse fly ash | 133.3 | [58] |
| Kaolin | 65.4 | [59] |
| Red clay | 125.0 | [8] |
| Peat | 265.4 | [60] |
| Saklıkent mud | 9.2 | [61] |
| *Artocarpus odoratissimus* peel | 174.0 | [62] |
| Watermelon rind | 92.6 | [63] |
| Cempedak durian peel | 98.0 | [12] |
| Modified or synthesized adsorbents | | |
| Mesoporous Ni-SBA-16 | 322.6 | [64] |
| Magnetite composite $Fe_3O_4$@SDBS@LDHs | 329.1 | [65] |
| Oxalic acid modified *Artocarpus odoratissimus* peel | 275.0 | [62] |
| Acid modified watermelon rind | 188.6 | [63] |
| Metaphosphoric acid modified cellulose | 150.0 | [66] |
| NaOH treated sawdust of Indian Eucalyptus wood | 58.5 | [67] |
| $ZnCl_2$ activated carbon from jute stick | 480.0 | [68] |
| Activated carbon from Acorn | 2.1 | [69] |
| ZnO nanoparticles on activated carbon | 142.9 | [70] |
| ZnS nanoparticles on activated carbon | 333.3 | [71] |
| Poly(acrylic acid) hydrogel composite | 24.9 | [14] |
| Binary oxidized cactus fruit peel | 166.7 | [72] |
| Hydrolyzed rice straw biochar | 111.1 | [73] |
| Phosphate cellulose with chloroethyl phosphate | 149.9 | [74] |

It must also be emphasized that MKL in this study has not undergone any modification, be it chemical or physical, but was only oven-dried at 60°C to remove water. Hence, further enhancement of its $q_{max}$ is still possible. Therefore, based on its high $q_{max}$ value as well as the possibility of enhancing its adsorption capacity, MKL poses a potential candidate as an adsorbent in the wastewater treatment process.

### 3.2.6. Thermodynamics studies

Thermodynamics studies are vital in providing crucial information which can aid in the design of wastewater treatment plant. The thermodynamics data can help determine if an adsorption takes place via an endothermic or exothermic process and whether it is spontaneous and favorable, using the Gibbs free energy as shown in Eq. (12) where $\Delta G°$, $\Delta H°$, and $\Delta S°$ are the Gibbs free energy, enthalpy change, and the entropy change, respectively and $T$ is the temperature in Kelvin (K). Further, the data obtained give useful information on the extensive property of the thermodynamics system understudied.

Investigation into the thermodynamics of the adsorption of BG by MKL was carried out at five different temperatures that is, 298, 313, 323, 333, and 343 K and the results are presented in Fig. 10. The data obtained were then fitted into the linear derivative of the Van't Hoff Eq. (14), which is a combination of Eq. (12) and the Gibbs free energy isotherm Eq. (13), where $K_c$ is the adsorption distribution coefficient, $C_s$ is the dye concentration at equilibrium (mg L$^{-1}$) being adsorbed, $C_e$ is the remaining dye concentration in

solution at equilibrium (mg $L^{-1}$), and $R$ is the gas constant (J $mol^{-1}$ $K^{-1}$).

$$\Delta G^\circ = \Delta H^\circ - T\Delta S^\circ \tag{12}$$

$$\Delta G^\circ = -RT \ln K_c \text{ where } K_c = \frac{C_S}{C_e} \tag{13}$$

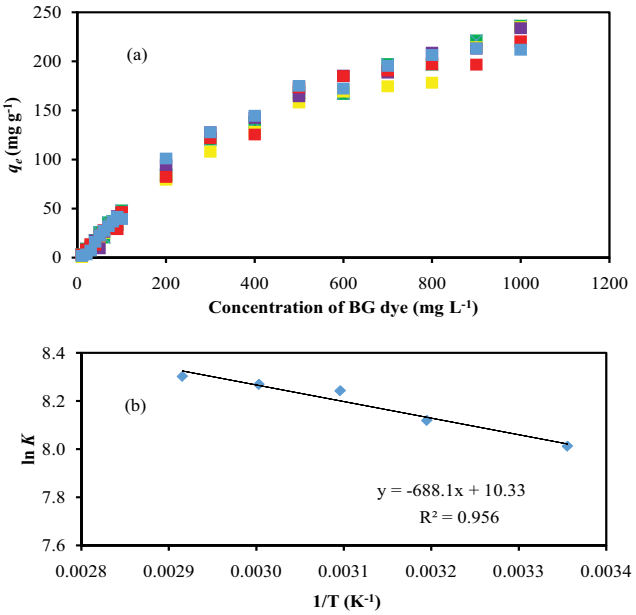


Fig. 10. (a) Investigation of adsorption thermodynamics of BG onto MKL at different temperatures [298 K (■), 313 K (■), 323 K (■), 333 K (■) and 343 K (■)] and (b) van Hoff's plot.

$$\ln k = \frac{\Delta S^\circ}{R} - \frac{\Delta H^\circ}{RT} \tag{14}$$

The thermodynamics data from Fig. 10 show that the adsorption of BG onto MKL was not affected much by the change in temperature. This was further confirmed by the $q_{max}$ values, shown in Table 5, showing not more than 11 mg $g^{-1}$ difference in their values over the range of temperature analyzed. The adsorption is an endothermic process with increased random disorder of the MKL-BG system based on the positive $\Delta H^\circ$ and $\Delta S^\circ$ values, respectively. Increasing temperature results in increasing negativity of the $\Delta G^\circ$ values which suggests a spontaneous adsorption process.

### 3.2.7. Regeneration and reusability of MKL

The investigation into the ability to regenerate and reuse MKL was carried out by using acid, base and distilled water treatments of the spent MKL together with a control for comparison purposes. The results displayed in Fig. 11 for both the control and washing with distilled water showed a drastic reduction in the spent MKL's adsorption capacity toward BG even in the first cycle. By the fifth cycle, the adsorbent practically could not adsorb anymore BG dye. Acid treatment of the spent MKL, although better than the control and washing with water, nevertheless showed more than 50% reduction of adsorption ability toward BG by the fifth cycle. Base treatment, on the other hand, showed promising results by maintaining high adsorption capacity even in the fifth cycle. This could be due to the base being able to remove surface fats and waxes on the adsorbent, thereby allowing functional groups to be more exposed to the adsorption of dye molecules. Further, the base can promote deprotonation thereby making the surface of the adsorbent

Table 5
Thermodynamics data for the adsorption of BG onto MKL

| Temperature ($K$) | $\Delta G^\circ$ (kJ $mol^{-1}$) | $\Delta S^\circ$ (J $mol^{-1}$ $K^{-1}$) | $\Delta H^\circ$ (kJ $mol^{-1}$) | ln$K$ | $1/T$ ($K^{-1}$) | $q_{max}$ (mg $g^{-1}$) |
|---|---|---|---|---|---|---|
| 298 | –19.85 | | | 8.012 | 0.0034 | 261.8 |
| 313 | –21.13 | | | 8.119 | 0.0032 | 254.4 |
| 323 | –22.13 | 85.89 | 5.72 | 8.242 | 0.0031 | 263.6 |
| 333 | –22.89 | | | 8.268 | 0.0030 | 252.6 |
| 343 | –23.67 | | | 8.302 | 0.0029 | 253.5 |

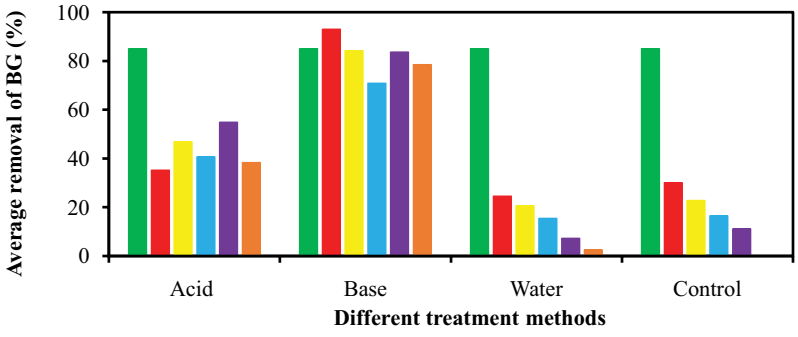


Fig. 11. Regeneration of spent MKL for the adsorption of BG in five consecutive cycles [Cycles 0 (■), 1 (■), 2 (■), 3 (■), 4 (■) and 5 (■)].

more negatively charged. BG being a cationic dye will, therefore, be more attracted to this negatively charged surface.

## 4. Conclusion

The results from this study indeed demonstrated that MKL, a new adsorbent, has great potential in its application for treating wastewater that contains BG dye. MKL exhibited high adsorption capacity with $q_{max}$ of 337.9 mg $g^{-1}$ based on the Sips isotherm model. The study also showed that the adsorbent has high tolerance when subject to changes in pH and salt solution. Thermodynamics data pointed to a spontaneous adsorption process and adsorption carried out at room temperature was sufficient to give a good $q_{max}$ value. MKL, being always available in large quantities throughout the year, is a great alternative low-cost adsorbent compared to other reported natural adsorbents. Moreover, the adsorbent showed great ability to be regenerated and reused especially in acid and base conditions. The rate of BG adsorption was also very fast, reaching equilibrium within half an hour. All these features further support MKL as an attractive absorbent to be applied in real-life wastewater treatment.

## Acknowledgements

Appreciation goes to the Government of Negara Brunei Darussalam, the Universiti Brunei Darussalam (UBD) for their continuous support and also to the Physical and Geology Sciences Program at UBD for the use of SEM.

## References

[1] R. Kant, Textile dyeing industry an environmental hazard, Nat. Sci., 4 (2012) 22–26.
[2] B. de Campos Ventura-Camargo, M.A. Marin-Morales, Azo dyes: characterization and toxicity-a Review, Text. Light Ind. Sci. Technol., 2 (2013) 85–103.
[3] V. Katheresan, J. Kansedo, S.Y. Lau, Efficiency of various recent wastewater dye removal methods: a review, J. Environ. Chem. Eng., 6 (2018) 4676–4697.
[4] S. De Gisi, G. Lofrano, M. Grassi, M. Notarnicola, Characteristics and adsorption capacities of low-cost sorbents for wastewater treatment: a review, Sustainable Mater. Technol., 9 (2016) 10–40.
[5] M.R.R. Kooh, M.K. Dahri, L.B.L. Lim, L.H. Lim, O.A. Malik, Batch adsorption studies of the removal of methyl violet 2B by soya bean waste: isotherm, kinetics and artificial neural network modeling, Environ. Earth Sci., 75 (2016) 783–797.
[6] R. Rehman, S. Farooq, T. Mahmud, Use of agro-waste *Musa acuminata* and *Solanum tuberosum* peels for economical sorptive removal of emerald green dye in ecofriendly way, J. Cleaner Prod., 206 (2019) 819–826.
[7] J. Mo, Q. Yang, N. Zhang, W. Zhang, Y. Zheng, Z. Zhang, A review on agro-industrial waste (AIW) derived adsorbents for water and wastewater treatment, J. Environ. Manage., 227 (2018) 395–405.
[8] M.S.U. Rehman, M. Munir, M. Ashfaq, N. Rashid, M.F. Nazar, M. Danish, J.I. Han, Adsorption of brilliant green dye from aqueous solution onto red clay, Chem. Eng. J., 228 (2013) 54–62.
[9] H.I. Chieng, L.B.L. Lim, N. Priyantha, D.T.B. Tennakoon, Sorption characteristics of peat of Brunei Darussalam III: equilibrium and kinetics studies on adsorption of crystal violet (CV), Int. J. Earth Sci. Eng., 6 (2013) 791–801.
[10] L.B.L. Lim, N. Priyantha, C.M. Chan, D. Matassan, H.I. Chieng, M.R.R. Kooh, Investigation of the sorption characteristics of water lettuce (WL) as a potential low-cost biosorbent for the removal of methyl violet 2B, Desal. Water Treat., 57 (2016) 8319–8329.
[11] F.S. Teodoro, M.M.C. Elias, G.M.D. Ferreira, O.F.H. Adarme, R.M.L. Savedra, M.F. Siqueira, L.V.A. Gurgel, Synthesis and application of a new carboxylated cellulose derivative. Part III: removal of auramine-O and safranin-T from mono- and bi-component spiked aqueous solutions, J. Colloid Interface Sci., 512 (2018) 575–590.
[12] M.K. Dahri, L.B.L. Lim, C.C. Mei, Cempedak durian as a potential biosorbent for the removal of brilliant green dye from aqueous solution: equilibrium, thermodynamics and kinetics studies, Environ. Monit. Assess., 187 (2015) 546–558.
[13] T. Zehra, N. Priyantha, L.B.L. Lim, Removal of crystal violet dye from aqueous solution using yeast-treated peat as adsorbent: thermodynamics, kinetics, and equilibrium studies, Environ. Earth Sci., 75 (2016) 35–371.
[14] S.R. Shirsath, A.P. Patil, R. Patil, J.B. Naik, P.R. Gogate, S.H. Sonawane, Removal of brilliant green from wastewater using conventional and ultrasonically prepared poly(acrylic acid) hydrogel loaded with kaolin clay: a comparative study, Ultrason. Sonochem., 20 (2013) 914–923.
[15] S. Srivastava, R. Sinha, D. Roy, Toxicological effects of malachite green, Aquat. Toxicol., 66 (2004) 319–329.
[16] M.R.K. Sheikh, F.I. Farouqui, P.R. Modak, A.M. Hoque, Z. Yasmin, Dyeing of Rajshahi silk with basic dyes: effect of modification on dyeing properties, J. Text. Inst., 97 (2006) 295–300.
[17] L.M. Goshman, Clinical toxicology of commercial products, J. Pharm. Sci., 74 (1985) 1139.
[18] M. Balabanova, L. Popova, R. Tchipeva, Dyes in dermatology, Disease-a-Month, 50 (2004) 270–279.
[19] W.M. Grant, C.C. Thomas, Toxicology of the eye, J. Toxicol. Cutaneous Ocul. Toxicol., 6 (1987) 155–156.
[20] M. Oplatowska, R.F. Donnelly, R.J. Majithiya, D. Glenn Kennedy, C.T. Elliott, The potential for human exposure, direct and indirect, to the suspected carcinogenic triphenylmethane dye brilliant green from green paper towels, Food Chem. Toxicol., 49 (2011) 1870–1876.
[21] M. Foroughi-Dahr, H. Abolghasemi, M. Esmaili, A. Shojamoradi, H. Fatoorehchi, Adsorption characteristics of congo red from aqueous solution onto tea waste, Chem. Eng. Commun., 202 (2015) 181–193.
[22] L.B.L. Lim, N. Priyantha, N.A.H. Mohamad Zaidi, A superb modified new adsorbent, *Artocarpus odoratissimus* leaves, for removal of cationic methyl violet 2B dye, Environ. Earth Sci., 75 (2016) 1179–1191.
[23] N. Nooraee Nia, M. Rahmani, M. Kaykhaii, M. Sasani, Evaluation of *Eucalyptus* leaves as an adsorbent for decolorization of Methyl Violet (2B) dye in contaminated waters: thermodynamic and kinetics model, Model. Earth Syst. Environ., 3 (2017) 825–829.
[24] L.B.L. Lim, N. Priyantha, Y. Lu, N.A.H. Mohamad Zaidi, Effective removal of methyl violet dye using pomelo leaves as a new low-cost adsorbent, Desal. Water Treat., 110 (2018) 264–274.
[25] L. Bulgariu, L.B. Escudero, O.S. Bello, M. Iqbal, J. Nisar, K.A. Adegoke, I. Anastopoulos, The utilization of leaf-based adsorbents for dyes removal: a review, J. Mol. Liq., 276 (2019) 728–747.
[26] T.K. Lim, *Dimocarpus longan* ssp. *malesianus* var. *malesianus*, Edible Medicinal and Non-medicinal Plants, Dordrecht, Springer Netherlands, 6 (2013) 33–38.
[27] S.M.N. Azmi, P. Jamal, A. Amid, Xanthine oxidase inhibitory activity from potential Malaysian medicinal plant as remedies for gout, Int. Food Res. J., 19 (2012) 59–66.
[28] N.A.H.M. Zaidi, L.B.L. Lim, A. Usman, Enhancing adsorption of malachite green dye using base-modified *Artocarpus odoratissimus* leaves as adsorbents, Environ. Technol. Innovation, 13 (2019) 211–223.
[29] H.I. Chieng, T. Zehra, L.B.L. Lim, N. Priyantha, D.T.B. Tennakoon, Sorption characteristics of peat of Brunei Darussalam IV: equilibrium, thermodynamics and kinetics of adsorption of methylene blue and malachite green dyes from aqueous solution, Environ. Earth Sci., 72 (2014) 2263–2277.
[30] N. Ayawei, A.N. Ebelegi, D. Wankasi, Modeling and interpretation of adsorption isotherms, J. Chem., 2017 (2017) 1–11.

[31] N. Akter, M.A. Hossain, M.J. Hassan, M.K. Amin, M. Elias, M.M. Rahman, M.A. Hasnat, Amine modified tannin gel for adsorptive removal of brilliant green dye, J. Environ. Chem. Eng., 4 (2016) 1231–1241.
[32] L.B.L. Lim, N. Priyantha, D.T.B. Tennakoon, H.I. Chieng, M.K. Dahri, M. Suklueng, Breadnut peel as a highly effective low-cost biosorbent for methylene blue: equilibrium, thermodynamic and kinetic studies, Arabian J. Chem., 10 (2017) 3216–3228.
[33] N.A.H. Mohamad Zaidi, W.J. Liew, L.B.L. Lim, Adsorption of brilliant green dye on *Nephelium mutabile* (Pulasan) leaves, Sci. Bruneiana, 17 (2018) 25–34.
[34] M. Nigam, S. Rajoriya, S. Rani Singh, P. Kumar, Adsorption of Cr (VI) ion from tannery wastewater on tea waste: kinetics, equilibrium, and thermodynamics studies, J. Environ. Chem. Eng., 7 (2019) 1–9.
[35] H. Chen, J. Zhao, G. Dai, J. Wu, H. Yan, Adsorption characteristics of Pb(II) from aqueous solution onto a natural biosorbent, fallen *Cinnamomum camphora* leaves, Desalination, 262 (2010) 174–182.
[36] M.R.R. Kooh, M.K. Dahri, L.B.L. Lim, Removal of methyl violet 2B dye from aqueous solution using *Nepenthes rafflesiana* pitcher and leaves, Appl. Water Sci., 7 (2017) 3859–3868.
[37] E. Suganya, N. Saranya, C. Patra, L.A. Varghese, N. Selvaraju, Biosorption potential of *Gliricidia sepium* leaf powder to sequester hexavalent chromium from synthetic aqueous solution, J. Environ. Chem. Eng., 7 (2019) 1–9.
[38] Y. Hu, T. Guo, X. Ye, Q. Li, M. Guo, H. Liu, Z. Wu, Dye adsorption by resins: effect of ionic strength on hydrophobic and electrostatic interactions, Chem. Eng. J., 228 (2013) 392–397.
[39] L.B.L. Lim, N. Priyantha, K.J. Mek, N.A.H.M. Zaidi, Potential use of *Momordica charantia* (Bitter gourd) waste as a low-cost adsorbent to remove toxic crystal violet dye, Desal. Water Treat., 82 (2017) 121–130.
[40] M.K. Dahri, H.I. Chieng, L.B.L. Lim, N. Priyantha, C.C. Mei, Cempedak durian (*Artocarpus* sp.) peel as a biosorbent for the removal of toxic methyl Violet 2B from aqueous solution, Korean Chem. Eng. Res, 53 (2015) 576–583.
[41] L.B.L. Lim, N. Priyantha, C.M. Chan, D. Matassan, H.I. Chieng, M.R.R. Kooh, Adsorption behavior of methyl violet 2B using duckweed: equilibrium and kinetics studies, Arabian J. Sci. Eng., 39 (2014) 6757–6765.
[42] S. Lagergren, About the theory of so-called adsorption of soluble substances, K. Sven. Vetenskapsakad. Handl., 24 (1898) 1–39.
[43] Y.S. Ho, G. McKay, Sorption of dye from aqueous solution by peat, Chem. Eng. J., 70 (1998) 115–124.
[44] W. Weber, J. Morris, Kinetics and adsorption on carbon from solution, J. Sanit. Eng. Div., 89 (1963) 31–60.
[45] B. Nagy, C. Manzatu, A. Maicaneanu, C. Indolean, L. Barbu-Tudoran, C. Majdik, Linear and nonlinear regression analysis for heavy metals removal using *Agaricus bisporus* macrofungus, Arabian J. Chem., 10 (2017) S3569–S3579.
[46] I. Langmuir, The adsorption of gases on plane surfaces of glass, mica and platinum, J. Am. Chem. Soc., 40 (1918) 1361–1403.
[47] H. Freundlich, Over the adsorption in the solution, J. Phys. Chem., 57 (1906) 385–470.
[48] M.J. Temkin, V. Pyzhev, Kinetics of ammonia synthesis on promoted iron catalysts, Acta Phys. Chim., 12 (1940) 217–222.
[49] O. Redlich, D.L. Peterson, A useful adsorption isotherm, J. Phys. Chem., 63 (1959) 1024.
[50] R. Sips, On the structure of a catalyst surface, J. Chem. Phys., 16 (1948) 490–495.
[51] R. Rehman, T. Mahmud, M. Irum, Brilliant green dye elimination from water using *Psidium guajava* leaves and *Solanum tuberosum* peels as adsorbents in environmentally benign way, J. Chem., 2015 (2015) 1–8.
[52] K. Bhattacharyya, Adsorption characteristics of the dye, Brilliant green, on Neem leaf powder, Dyes Pigm., 57 (2003) 211–222.
[53] A. Sharma, K.G. Bhattacharyya, Utilization of a biosorbent based on *Azadirachta indica* (Neem) leaves for removal of water-soluble dyes, Indian J. Chem. Technol., 12 (2005) 285–295.
[54] N. Gupta, A.K. Kushwaha, M.C. Chattopadhyaya, Adsorption studies of cationic dyes onto Ashoka (*Saraca asoca*) leaf powder, J. Taiwan Inst. Chem. Eng., 43 (2012) 604–613.
[55] J. Anwar, R. Rehman, T. Mahmud, M. Salman, Isothermal modeling of batch biosorption of brilliant green dye from water by chemically modified *Eugenia jambolana* leaves, J. Chem. Soc. Pak., 34 (2012) 136–143.
[56] V.S. Mane, I. Deo Mall, V. Chandra Srivastava, Kinetic and equilibrium isotherm studies for the adsorptive removal of brilliant green dye from aqueous solution by rice husk ash, J. Environ. Manage., 84 (2007) 390–400.
[57] M.K. Dahri, M.R.R. Kooh, L.B.L. Lim, Adsorption characteristics of pomelo skin toward toxic brilliant green dye, Sci. Bruneiana, 16 (2017) 49–56.
[58] V.S. Mane, I.D. Mall, V.C. Srivastava, Use of bagasse fly ash as an adsorbent for the removal of brilliant green dye from aqueous solution, Dyes Pigm., 73 (2007) 269–278.
[59] B.K. Nandi, A. Goswami, M.K. Purkait, Adsorption characteristics of brilliant green dye on kaolin, J. Hazard. Mater., 161 (2009) 387–395.
[60] H.I. Chieng, N. Priyantha, L.B.L. Lim, Effective adsorption of toxic brilliant green from aqueous solution using peat of Brunei Darussalam: isotherms, thermodynamics, kinetics and regeneration studies, RSC Adv., 5 (2015) 34603–34615.
[61] Y. Kismir, A.Z. Aroguz, Adsorption characteristics of the hazardous dye brilliant green on Saklıkent mud, Chem. Eng. J., 172 (2011) 199–206.
[62] M.K. Dahri, L.B.L. Lim, M.R.R. Kooh, C.M. Chan, Adsorption of brilliant green from aqueous solution by unmodified and chemically modified Tarap (*Artocarpus odoratissimus*) peel, Int. J. Environ. Sci. Technol., 14 (2017) 2683–2694.
[63] R. Lakshmipathy, N.A. Reddy, N.C. Sarada, Optimization of brilliant green biosorption by native and acid-activated watermelon rind as low-cost adsorbent, Desal. Water Treat., 54 (2015) 235–244.
[64] A.T. Shah, M.I. Din, F.N. Kanwal, M.L. Mirza, Direct synthesis of mesoporous molecular sieves of Ni-SBA-16 by internal pH adjustment method and its performance for adsorption of toxic brilliant green dye, Arabian J. Chem., 8 (2015) 579–586.
[65] D. Zhang, M. Zhu, J. Yu, H. Meng, F. Jiao, Effective removal of brilliant green from aqueous solution with magnetic $Fe_3O_4$@SDBS@LDHs composites, Trans. Nonferrous Met. Soc. China, 27 (2017) 2673–2681.
[66] F. de Castro Silva, M.M.F. da Silva, L.C.B. Lima, J.A. Osajima, E.C. da Silva Filho, Modifying cellulose with metaphosphoric acid and its efficiency in removing brilliant green dye, Int. J. Biol. Macromol., 114 (2018) 470–478.
[67] V.S. Mane, P.V.V. Babu, Studies on the adsorption of brilliant green dye from aqueous solution onto low-cost NaOH treated sawdust, Desalination, 273 (2011) 321–329.
[68] M. Asadullah, M. Asaduzzaman, M.S. Kabir, M.G. Mostofa, T. Miyazawa, Chemical and structural evaluation of activated carbon prepared from jute sticks for brilliant green dye removal from aqueous solution, J. Hazard. Mater., 174 (2010) 437–443.
[69] M. Ghaedi, H. Hossainian, M. Montazerozohori, A. Shokrollahi, F. Shojaipour, M. Soylak, M.K. Purkait, A novel acorn based adsorbent for the removal of brilliant green, Desalination, 281 (2011) 226–233.
[70] M. Ghaedi, G. Negintaji, H. Karimi, F. Marahel, Solid-phase extraction and removal of brilliant green dye on zinc oxide nanoparticles loaded on activated carbon: new kinetic model and thermodynamic evaluation, J. Ind. Eng. Chem., 20 (2014) 1444–1452.
[71] M. Ghaedi, A. Ansari, F. Bahari, A.M. Ghaedi, A. Vafaei, A hybrid artificial neural network and particle swarm optimization for prediction of removal of hazardous dye brilliant green from aqueous solution using zinc sulfide nanoparticle loaded on activated carbon, Spectrochim. Acta, Part A, 137 (2015) 1004–1015.
[72] R. Kumar, M.A. Barakat, Decolourization of hazardous brilliant green from aqueous solution using binary oxidized cactus fruit peel, Chem. Eng. J., 226 (2013) 377–383.
[73] M. Saif Ur Rehman, I. Kim, N. Rashid, M. Adeel Umer, M. Sajid, J.-I. Han, Adsorption of brilliant green dye on biochar prepared from lignocellulosic bioethanol plant waste, CLEAN – Soil Air Water, 44 (2016) 55–62.
[74] F. de Castro Silva, M.M.F. da Silva, L.C.B. Lima, J.A. Osajima, E.C. da Silva Filho, Integrating chloroethyl phosphate with biopolymer cellulose and assessing their potential for absorbing brilliant green dye, J. Environ. Chem. Eng., 4 (2016) 3348–3356.